



HAL
open science

On the Digital Control of MEMS Gyroscopes: a Robust Approach

Fabricio Saggin, Cécile Pernin, Anton Korniienko, Gérard Scorletti,
Christophe Le Blanc

► **To cite this version:**

Fabricio Saggin, Cécile Pernin, Anton Korniienko, Gérard Scorletti, Christophe Le Blanc. On the Digital Control of MEMS Gyroscopes: a Robust Approach. [Research Report] Ecole Centrale de Lyon. 2021. hal-03125932v1

HAL Id: hal-03125932

<https://hal.science/hal-03125932v1>

Submitted on 29 Jan 2021 (v1), last revised 8 Feb 2021 (v2)

HAL is a multi-disciplinary open access archive for the deposit and dissemination of scientific research documents, whether they are published or not. The documents may come from teaching and research institutions in France or abroad, or from public or private research centers.

L'archive ouverte pluridisciplinaire **HAL**, est destinée au dépôt et à la diffusion de documents scientifiques de niveau recherche, publiés ou non, émanant des établissements d'enseignement et de recherche français ou étrangers, des laboratoires publics ou privés.

On the Digital Control of MEMS Gyroscopes: a Robust Approach

Fabrício Saggin*, Cécile Pernin*, Anton Korniienko*, Gérard Scorletti* and Christophe Le Blanc†

* Laboratoire Ampère, Ecole Centrale de Lyon, Université de Lyon, France

† Asygn, Grenoble, France

I. ABSTRACT

This document provides further details on the paper “Digital Control of MEMS Gyroscopes: a Robust Approach” [1]. These details concern the choice of the weighting functions for the H_∞ synthesis.

II. PROBLEM STATEMENT

As described in [1], the object of study is the control of a MEMS gyroscope.

The considered control architecture is represented in Fig. 1, where G_c is the model of the gyroscope with actuation and instrumentation, and K_c is the controller. Both are Multi Input Multi Output (MIMO) systems, in continuous time (CT). The controller K_c applies a signal u_x (resp. u_y) on the drive (resp. sense) mode. The signal d_x (resp. d_y) is the disturbance on u_x (resp. u_y) and is used to represent the Coriolis force acting on the drive mode (resp. from the drive to the sense mode). Thus, estimating d_y allows to compute the Coriolis force, and then the angular rate. The input signals of G_c are u_{d_x} and u_{d_y} . The outputs of G_c are the displacements on the drive mode x and on the sense mode y . The measurement noise is denoted n_x (resp. n_y) on the drive (resp. sense) mode. ω_{0_x} (resp. ω_{0_y}) is the drive (resp. sense) resonance frequency (in rad/s).

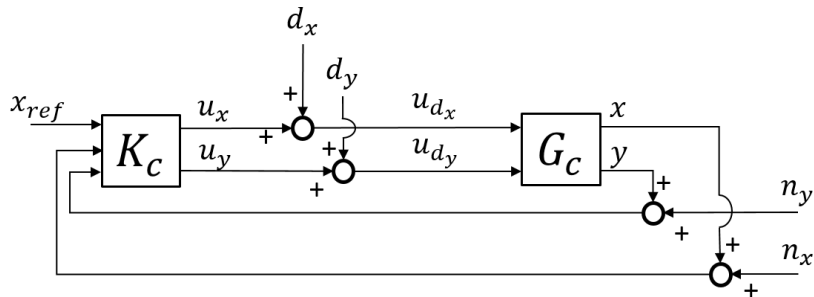


Fig. 1: Control architecture

A model of the gyroscope, G_c , is obtained by identification and the electrical coupling is compensated, as described in [2], [3]. Its Bode diagram of the gyroscope is presented in Fig. 2 and G_c is partitioned as follows:

$$G_c(s) = \begin{bmatrix} G_{xx}(s) & G_{xy}(s) \\ G_{yx}(s) & G_{yy}(s) \end{bmatrix}, \quad (1)$$

where the main dynamics of G_{xx} (resp. G_{yy}) corresponds to a resonator with resonance frequency ω_{0_x} (resp. ω_{0_y}) and quality factor Q_x (resp. Q_y), presented in Table I. The transfers G_{xy} and G_{yx} model the couplings between drive and sense modes. The transfer G_{yx} presents resonance peaks at ω_{0_x} and ω_{0_y} and a magnitude that is globally smaller than that of G_{xx} and G_{yy} . The transfer G_{xy} is negligible. Finally, the actuation and instrumentation circuitry justifies the phase of the transfers.

TABLE I: Main characteristics of the MEMS gyroscope

ω_{0_x} (rad/s)	ω_{0_y} (rad/s)	Q_x	Q_y
$2\pi \cdot 11586$	$2\pi \cdot 11677$	80502	8099

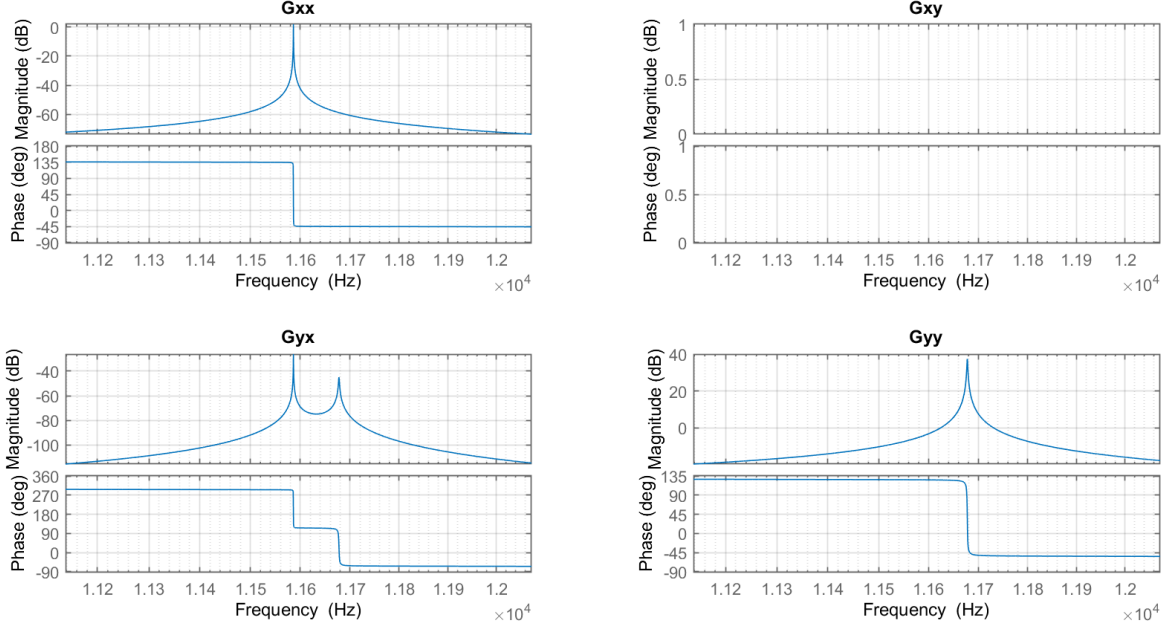


Fig. 2: Bode diagram of the gyroscope model.

The main control specifications are :

- 1) Track the sinusoidal reference signal $x_{ref}(t) = A_{ref} \sin(\omega_{0_x} t)$ with an error $\varepsilon_x(t) = x_{ref}(t) - x(t)$, such that $|\varepsilon_x| < \varepsilon_{x_{max}} A_{ref}$ in steady-state, where $A_{ref} \in \mathbb{R}$ and $\varepsilon_{x_{max}} \in \mathbb{R}^+$.
- 2) Reject the disturbance $d_y(t) = A_{d_y} \sin(\omega_{0_x} t + \phi_y)$ on the signal u_{d_y} , i.e., with an error u_{d_y} such that $|u_{d_y}| < \varepsilon_{u_{d_y_{max}}} A_{d_y}$, where $A_{d_y} \in \mathbb{R}$, $\phi_y \in \mathbb{R}$ and $\varepsilon_{u_{d_y_{max}}} \in \mathbb{R}^+$.

Secondary control objectives are also considered:

- Minimize the control effort u_x on the drive mode.
- Limit the influence of the measurement noises n_x and n_y .
- Reject the disturbance $d_x(t) = A_{d_x} \sin(\omega_{0_x} t + \phi_x)$ with an error $\varepsilon'_x(t) = x(t)$, such that $|\varepsilon'_x| < \varepsilon'_{x_{max}} A_{d_x}$ in steady-state, where $A_{d_x} \in \mathbb{R}$, $\phi_x \in \mathbb{R}$ and $\varepsilon'_{x_{max}} \in \mathbb{R}^+$.

III. CHOICE OF THE WEIGHTING FUNCTION PARAMETERS

In the H_∞ synthesis, the controller design is formulated as an optimization problem subject to mathematical constraints, which express performance and stability robustness requirements into a mathematical criterion to be minimized. The choice of the input and output signals and of the weighting functions, the so-called H_∞ criterion, must be adapted to the specifications.

We consider the criterion presented in Fig. 3, where the signals of interest $\tilde{w} = (x_{ref}, d_x, d_y, n_x, n_y)^T$ and $\tilde{z} = (\varepsilon_x, u_x, u_{d_y})^T$, weighting functions $W_w = \text{diag}(W_{w_1}, \dots, W_{w_5})$ and $W_z = \text{diag}(W_{z_1}, \dots, W_{z_3})$ are defined with $w = W_w^{-1} \tilde{w}$ and $z = W_z \tilde{z}$.

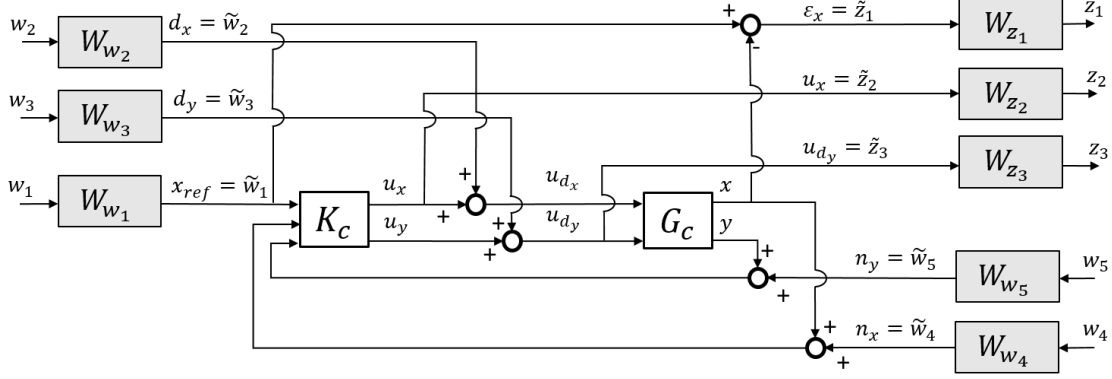


Fig. 3: H_∞ criterion

The H_∞ problem is the following: for a given γ , find a controller such that the weighted closed-loop transfer functions are stable and

$$\left\| \begin{bmatrix} T_{w_1 \rightarrow z_1} & T_{w_2 \rightarrow z_1} & T_{w_3 \rightarrow z_1} & T_{w_4 \rightarrow z_1} & T_{w_5 \rightarrow z_1} \\ T_{w_1 \rightarrow z_2} & T_{w_2 \rightarrow z_2} & T_{w_3 \rightarrow z_2} & T_{w_4 \rightarrow z_2} & T_{w_5 \rightarrow z_2} \\ T_{w_1 \rightarrow z_3} & T_{w_2 \rightarrow z_3} & T_{w_3 \rightarrow z_3} & T_{w_4 \rightarrow z_3} & T_{w_5 \rightarrow z_3} \end{bmatrix} \right\|_\infty < \gamma, \quad (2)$$

where we use the notation $T_{a \rightarrow b}$ to denote the transfer from a signal a to a signal b .

If the above problem has a solution with $\gamma < 1$, then it can be shown (see [4]) that (2) implies

$$\forall \omega \in \mathbb{R}, \forall k \in \{1, \dots, 5\}, \forall l \in \{1, \dots, 3\}, |T_{\tilde{w}_k \rightarrow \tilde{z}_l}(j\omega)| < |W_{w_k}(j\omega)W_{z_l}(j\omega)|^{-1}. \quad (3)$$

Therefore, the choice of the weighting functions allows imposing upper bounds on the magnitude of the closed-loop transfer functions and thus to ensure compliance with the specifications, which are themselves expressed as upper bounds objectives.

Two main types of weighting functions were used in this work, which are adapted to the reference tracking and disturbance rejection of sinusoidal signals [5]:

- 1) An ‘‘amplification’’ weighting function W_{amp}

$$W_{amp}(k, W_{max}, W_{int}, \omega_{min}, \omega_{max}, s) = k \cdot \frac{s^2 + \alpha s + \omega_{min}\omega_{max}}{s^2 + \alpha/W_{max} \cdot s + \omega_{min}\omega_{max}} \quad (4)$$

with

$$\alpha = (\omega_{max} - \omega_{min}) \cdot W_{max} \cdot \sqrt{\frac{W_{int}^2 - 1}{W_{max}^2 - W_{\omega}^2}}, \quad (5)$$

where $k > 0$, $W_{max} > W_{int} > 0$ and $\omega_{max} > \omega_{min} > 0$ can be chosen by the user. The magnitude plot of this type of weighting function is given in Fig. 4, with $\omega_0^2 = \omega_{min} \cdot \omega_{max}$.

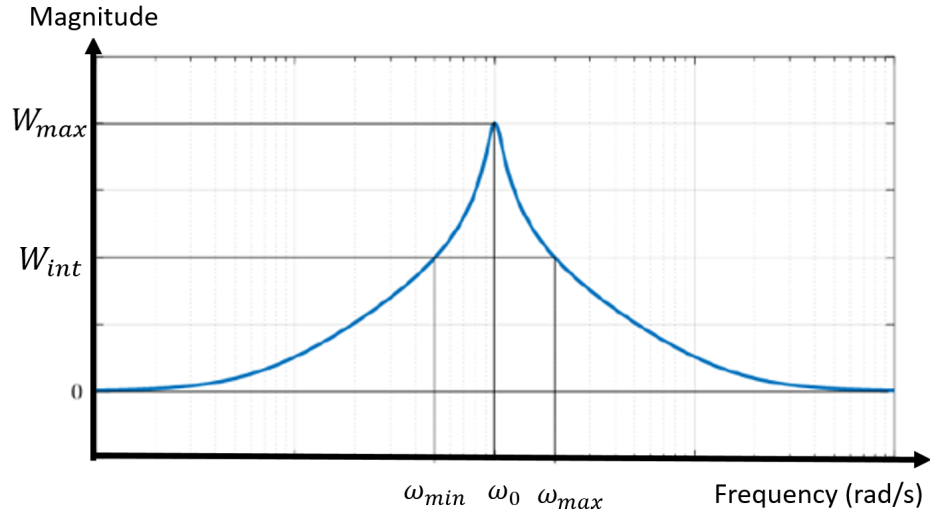


Fig. 4: Magnitude plot of W_{amp}

2) An “attenuation” weighting function W_{att}

$$W_{att}(k, W_{min}, W_{int}, \omega_{min}, \omega_{max}, s) = k \cdot \frac{s^2 + \beta W_{min} s + \omega_{min} \omega_{max}}{s^2 + \beta s + \omega_{min} \omega_{max}} \quad (6)$$

with

$$\beta = (\omega_{max} - \omega_{min}) \cdot \sqrt{\frac{1 - W_{int}^2}{W_{int}^2 - W_{max}^2}} \quad (7)$$

The magnitude of this transfer is given in Fig. 5, with $\omega_0^2 = \omega_{min} \cdot \omega_{max}$.

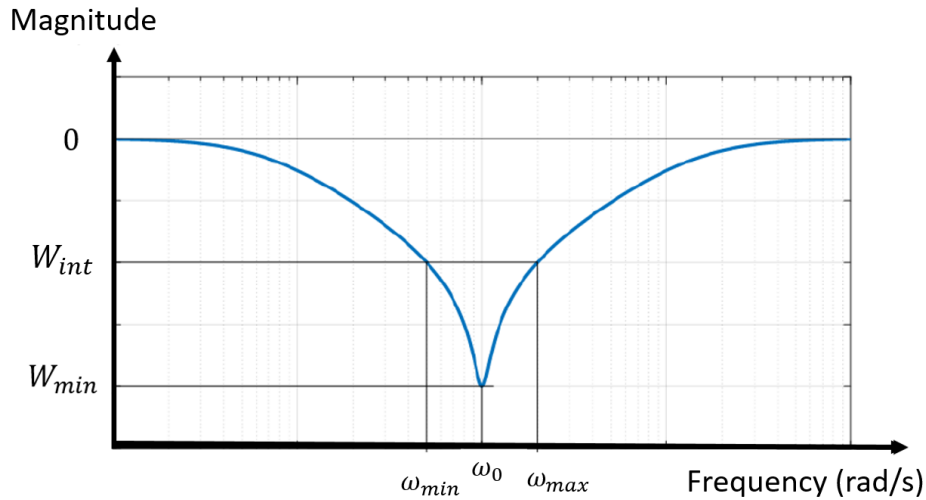


Fig. 5: Magnitude plot of W_{att}

The desired specifications can be expressed through the choice of the weighting functions and their parameters, as follows.

Main Control Specifications

- Reference tracking:

The signals of interest are x_{ref} , the reference signal, and ε_x , the tracking error to be minimized. The function to be worked on is $T_{x_{ref} \rightarrow \varepsilon_x}$. The objective is to track a sinusoidal reference signal x_{ref} of frequency ω_{0_x} . More precisely, the first control specification demands:

$$\left| T_{x_{ref} \rightarrow \varepsilon_x}(j\omega_{0_x}) \right| < \varepsilon_{x_{max}} \quad (8)$$

For $k = l = 1$, (3) is equivalent to

$$\forall \omega \in \mathbb{R}, \left| T_{x_{ref} \rightarrow \varepsilon_x}(j\omega) \right| < |W_{z_1}(j\omega)W_{w_1}(j\omega)|^{-1}. \quad (9)$$

Thus, (8) can be enforced using (9) via the product $W_{\varepsilon_x}W_{x_{ref}}$. The weighting functions must be chosen so that $|W_{w_1}(j\omega_{0_x})W_{z_1}(j\omega_{0_x})|^{-1} \leq \varepsilon_{x_{max}}$.

The weighting functions are retained such that:

$$W_{w_1} \cdot W_{z_1} = W_{amp}(k_1, W_{max_1}, W_{int_1}, \omega_{min_1}, \omega_{max_1}) \quad (10)$$

with

$$\begin{cases} \omega_{max_1} = \omega_{0_x} + \delta\omega_x \\ \omega_{min_1} = \omega_{0_x} - \delta\omega_x, \\ W_{int_1} = \frac{1}{\varepsilon_{x_{max}} \cdot k_1} \end{cases} \quad (11)$$

where $\delta\omega_x > 0$ is associated with the reference tracking bandwidth, $k_1 > 0$ and $W_{max_1} > 0$. In general, these parameters are chosen by the user iteratively.

- *Disturbance rejection on the sense mode:*

The signals of interest are d_y , the disturbance, and u_{d_y} , the estimation error to be minimized. The function to be worked on is $T_{d_y \rightarrow u_{d_y}}$. The second control specification demands:

$$\left| T_{d_y \rightarrow u_{d_y}}(j\omega_{0_x}) \right| < \varepsilon_{u_{d_y_{max}}} \quad (12)$$

With $k = l = 3$, (3) is equivalent to

$$\forall \omega \in \mathbb{R}, \left| T_{d_y \rightarrow u_{d_y}}(j\omega) \right| < |W_{w_3}(j\omega)W_{z_3}(j\omega)|^{-1}. \quad (13)$$

Similar to the reference tracking, the weighting functions are such that:

$$W_{w_3} \cdot W_{z_3} = W_{amp}(k_2, W_{max_2}, W_{int_2}, \omega_{min_2}, \omega_{max_2}) \quad (14)$$

with

$$\begin{cases} \omega_{max_1} = \omega_{0_x} + \delta\omega_y \\ \omega_{min_1} = \omega_{0_x} - \delta\omega_y, \\ W_{int_2} = \frac{1}{\varepsilon_{u_{d_y_{max}}} \cdot k_2} \end{cases} \quad (15)$$

where $\delta\omega_y > 0$ is associated with the bandwidth of the disturbance rejection on the sense mode, $k_2 > 0$ and $W_{max_2} > 0$. In general, these parameters are chosen by the user iteratively.

Secondary Control Specifications

- *Minimization of the control effort on the drive mode.*

The signal of interest is u_x . All the transfer functions which have u_x as output signal are considered, but here, we focus on $T_{x_{ref} \rightarrow u_x}$, corresponding to the control effort to track the sinusoidal reference on the drive mode. Equation (3) implies that

$$\forall \omega \in \mathbb{R}, \left| T_{x_{ref} \rightarrow u_x}(j\omega) \right| < |W_{w_1}(j\omega)W_{z_2}(j\omega)|^{-1} \quad (16)$$

The gain of $T_{x_{ref} \rightarrow u_x}$ at ω_{0_x} is constrained by the specification of tracking (i.e. the value of $\varepsilon_{x_{max}}$) and the gains of the gyroscope at ω_{0_x} : $T_{x_{ref} \rightarrow u_x}(j\omega_{0_x})$ cannot be lowered under a

minimal value, necessary to ensure the reference tracking. This means that the control effort can only be influenced to a limited extent in steady state. This reasoning is actually valid not only at ω_{0_x} , but also for frequencies around ω_{0_x} , due to the bandwidth, associated with $\delta\omega_x$. However, it is possible to limit the control effort in transient state by minimizing as much as possible the gain of $T_{x_{ref} \rightarrow u_x}(j\omega)$ outside the bandwidth $[\omega_{0_x} - \delta\omega_x; \omega_{0_x} + \delta\omega_x]$. This also enforces the robust stability [4]. The weighting functions are chosen so that $W_{w_1} \cdot W_{z_2}$ behaves like an attenuation function, that is, with low gains around ω_{0_x} and high gains in low and high frequencies.

- *Limit the influence of the measurement noises n_x and n_y*
The signals of interests are n_x and n_y . Similarly to the control effort minimization, the weighting functions should be designed to minimize the magnitude of the transfer functions that have n_x and n_y as inputs. Again, trade-offs have to be made between the desired precision (reference tracking and disturbance rejection) and noise attenuation/limitation. Similarly to the control effort u_x , the weighting functions related to the signals n_x and n_y are chosen so that the transfer functions having n_x and n_y as inputs behave similar attenuation functions, that is, they have low gains around ω_{0_x} and high gains in low and high frequencies.
- *Disturbance rejection on the drive mode*
The disturbance d_x represents the Coriolis force acting on the drive mode. The reasoning is the same as for the disturbance rejection on the sense mode, and the weighting functions be chosen like:

$$W_{w_2} \cdot W_{z_1} = W_{amp}(k_3, W_{max_3}, W_{int_3}, \omega_{min_3}, \omega_{max_3}) \quad (17)$$

with

$$\begin{cases} \omega_{max_3} = \omega_{0_x} + \delta\omega'_x \\ \omega_{min_3} = \omega_{0_x} - \delta\omega'_x \\ W_{int_3} = \frac{1}{\varepsilon'_{x_{max}} \cdot k_3} \end{cases}, \quad (18)$$

where $\delta\omega'_x > 0$ is associated with the bandwidth of the disturbance rejection on the drive mode, $\varepsilon'_{x_{max}}$ corresponds to the disturbance rejection error, $k_3 > 0$ and $W_{max_1} > 0$. In general, these parameters are chosen by the user iteratively.

The final choice of the weighting functions is made keeping in mind that the more important the total order of the weighting functions is, the more important the order of the controller is.

The following numerical values are retained:

$$\begin{cases} \varepsilon_{x_{max}} = 0.005 \\ \delta\omega_x = 2 \text{ rad/s} \\ \varepsilon_{u_{dy_{max}}} = 0.02 \\ \delta\omega_y = 7 \text{ rad/s} \\ \varepsilon'_{x_{max}} = 0.005 \\ \delta\omega'_x = 2 \text{ rad/s} \end{cases} \quad (19)$$

The retained weighting functions are the following:

$$\left\{ \begin{array}{l} W_{w_1} = W_{amp}(k_1, W_{max_1}, W_{int_1}, \omega_{min_1}, \omega_{max_1}) \\ W_{w_2} = W_{amp}(k_3, W_{max_3}, W_{int_3}, \omega_{min_3}, \omega_{max_3}) \\ W_{w_3} = W_{amp}(k_2, W_{max_2}, W_{int_2}, \omega_{min_2}, \omega_{max_2}) \\ \quad W_{z_1} = 1 \\ W_{z_2} = W_{att}(k_4, W_{min_4}, W_{int_4}, \omega_{min_4}, \omega_{max_4}) \\ \quad W_{z_3} = 1 \\ W_{z_4} = W_{att}(k_5, W_{min_5}, W_{int_5}, \omega_{min_5}, \omega_{max_5}) \\ W_{z_5} = W_{att}(k_6, W_{min_6}, W_{int_6}, \omega_{min_6}, \omega_{max_6}) \end{array} \right. \quad (20)$$

All the parameters of these functions are given in Table II.

TABLE II: Numerical values of the parameters of the weighting functions

k_1	k_2	k_3	k_4	k_5	k_6
$10^{-8/20}$	$10^{-8/20}$	$10^{-8/20}$	$10^{40/20}$	$10^{80/20}$	$10^{40/20}$
W_{int_1}	W_{int_2}	W_{int_3}	W_{int_4}	W_{int_5}	W_{int_6}
$1/(\varepsilon_{x_{max}} \cdot k_1)$	$1/(\varepsilon_{u_{d_{y_{max}}}} \cdot k_2)$	$1/(\varepsilon'_{x_{max}} \cdot k_3)$	0.001	0.0178	0.224
W_{max_1}	W_{max_2}	W_{max_3}	W_{min_4}	W_{min_5}	W_{min_6}
$4 \cdot W_{int_1}$	$5 \cdot W_{int_2}$	$4 \cdot W_{int_3}$	10^{-5}	$5.6234 \cdot 10^{-5}$	$10^{40/20}$
ω_{min_1}	ω_{min_2}	ω_{min_3}	ω_{min_4}	ω_{min_5}	ω_{min_6}
$\omega_{0_x} - \delta\omega_x$	$\omega_{0_x} - \delta\omega_y$	$\omega_{0_x} - \delta\omega'_x$	0.6	0.75	0.9
ω_{max_1}	ω_{max_2}	ω_{max_3}	ω_{max_4}	ω_{max_5}	ω_{max_6}
$\omega_{0_x} + \delta\omega_x$	$\omega_{0_x} + \delta\omega_y$	$\omega_{0_x} + \delta\omega'_x$	1.6667	1.333	1.111

IV. SYNTHESIS RESULTS

With the model G_c and the weighting functions of the previous section, the H_∞ problem (see (2)) is solved with $\gamma = 0.95$. The closed-loop transfer functions are presented in Fig. 8 and Fig. 9. The upper bounds imposed by the weighting functions are respected.

The magnitude of $T_{x_{ref} \rightarrow \varepsilon_x}$ is low at the resonance frequency ω_{0_x} : -68 dB ($4 \cdot 10^{-4}$) $< \varepsilon_{x_{max}}$. Then, the tracking specification is respected.

The magnitude of $T_{d_x \rightarrow \varepsilon_x}$ is low at the resonance frequency ω_{0_x} : -50 dB ($3 \cdot 10^{-3}$) $< \varepsilon'_{x_{max}}$. Then, the disturbance rejection specification on the drive mode is respected.

The magnitude of $T_{d_y \rightarrow u_{d_y}}$ is low at the resonance frequency ω_{0_x} : -55 dB ($2 \cdot 10^{-3}$) $< \varepsilon_{u_{d_{y_{max}}}}$. Then, the disturbance rejection specification on the sense mode is respected.

The magnitude of the transfers with the noises n_x and n_y as inputs is minimized in low and high frequencies, limiting the influence of the measurement noises on the signals of interest.

The Bode plot of the obtained controller K_c is represented in Fig. 6 and Fig. 7. It is reminded that $In(1)$, or $Input(1)$, is x_{ref} ; $In(2)$ is x ; $In(3)$ is y ; $Out(1)$ is u_x ; $Out(2)$ is u_y . The controller has important gains around the resonance frequency ω_{0_x} , which enables to ensure a good tracking of x_{ref} and a good estimation of d_y . Its gains are weak in low and high frequencies, which enables to minimize the control effort in transient state, the influence of the measurement noise on the signals of interest, and enhancement of the robustness.

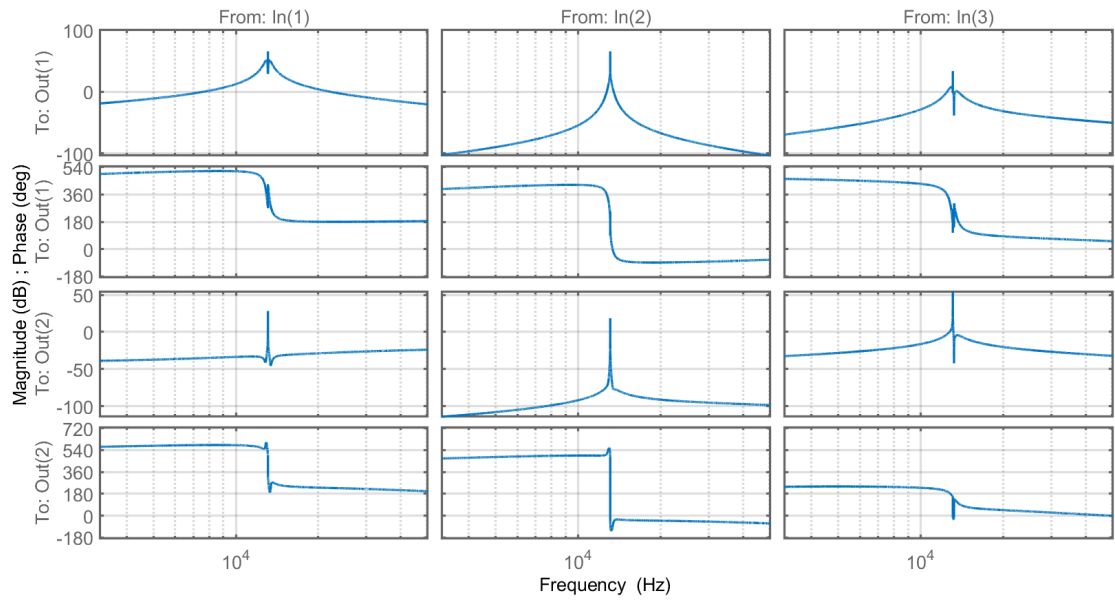


Fig. 6: Bode plot of K_c

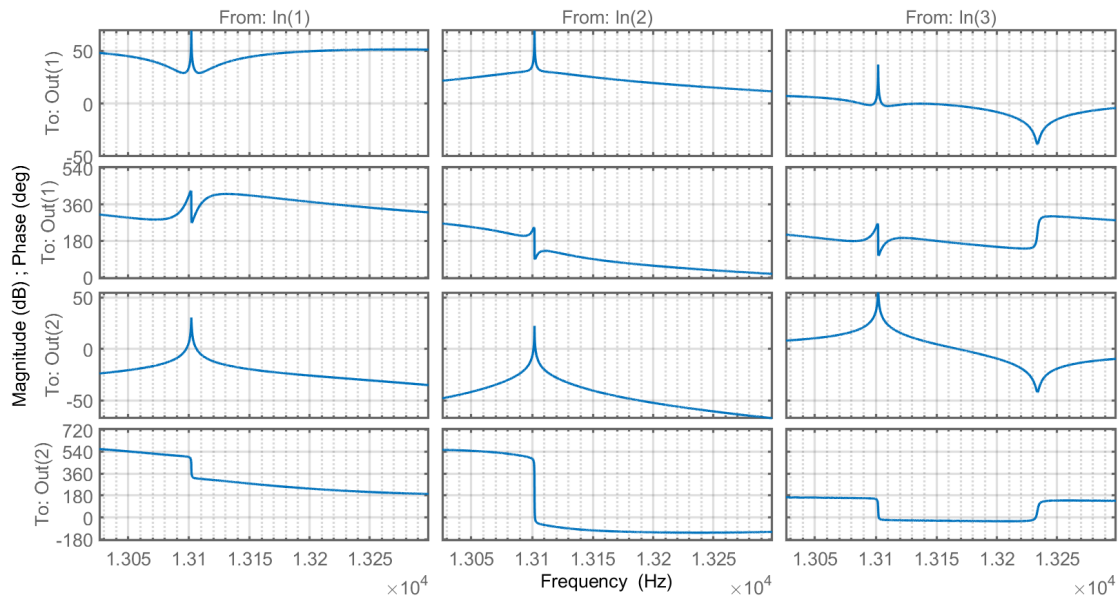


Fig. 7: Bode plot of K_c – zoom

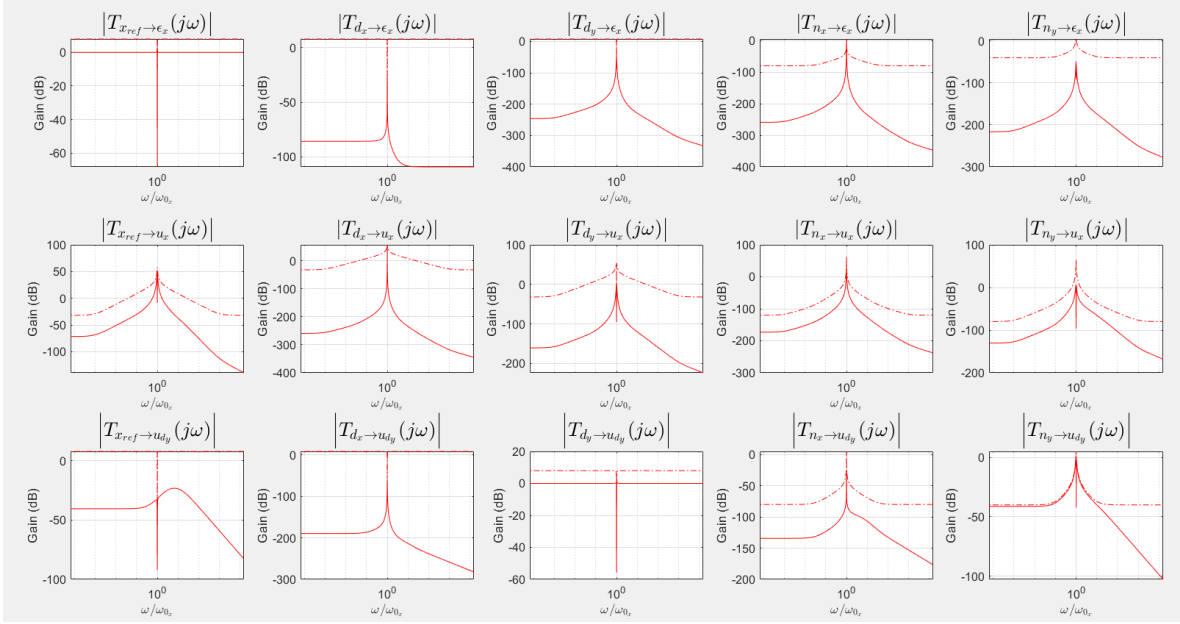


Fig. 8: Magnitudes of the closed-loop transfer functions (solid line) and upper bounds enforced by the weighting functions (dashed line).

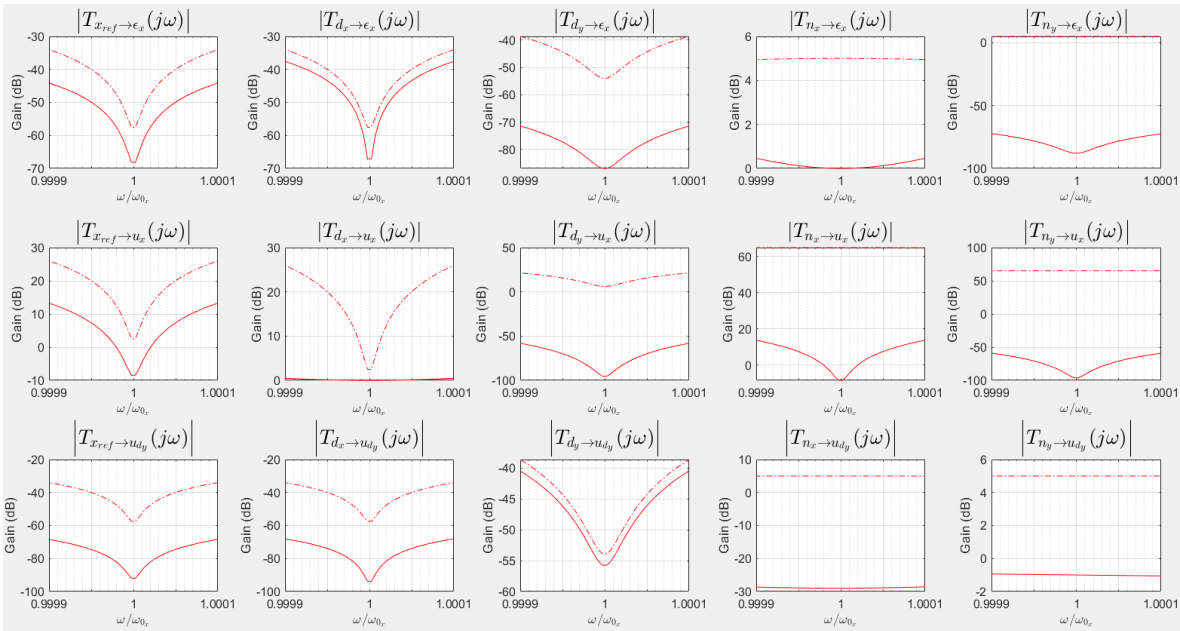


Fig. 9: Zoom around ω_{0_x} on the magnitudes of the closed-loop transfer functions (solid line) and upper bounds enforced by the weighting functions (dashed line).

REFERENCES

- [1] F. Saggini, C. Pernin, A. Korniienko, G. Scorletti, and C. Le Blanc, "Digital Control of MEMS Gyroscopes: a Robust Approach," in *IEEE International Symposium on Inertial Sensors and Systems (INERTIAL)*. (to be published), 2021.
- [2] K. Colin, F. Saggini, C. Le Blanc, X. Bombois, A. Korniienko, and G. Scorletti, "Identification-Based Approach for Electrical Coupling Compensation in a MEMS Gyroscope," in *IEEE International Symposium on Inertial Sensors and Systems (INERTIAL)*. IEEE, apr 2019, pp. 1–4.

- [3] K. Colin, "Data informativity for the prediction error identification of MIMO systems : identification of a MEMS gyroscope," Theses, Université de Lyon, Sep. 2020. [Online]. Available: <https://tel.archives-ouvertes.fr/tel-03114994>
- [4] S. Skogestad and I. Postlethwaite, *Multivariable feedback control - analysis and design*, 2nd ed. John Wiley & Sons, 2001.
- [5] G. Scorletti and V. Fromion, *Automatique fréquentielle avancée*, 2009. [Online]. Available: <https://cel.archives-ouvertes.fr/cel-00423848v2>